BIOCELL

Tech Science Press

http://doi.org/10.32604/biocell.2026.081166

ARTICLE

Low Expression of ARHGAP40 in Colorectal Cancer Facilitates Tumor Progression by Activating the RhoA Pathway

Bin Lian[1,2,#], Na You[2,3,#], Jingyu Wang[4], Cong Wang[4], Yunjie Wen[2] and Jiandong Wang[5,*]

[1]School of Medicine, Nanjing University, Nanjing, China
[2]Guangzhou Huayin Medical Laboratory Center Co., Ltd., Guangzhou, China
[3]School of Biology and Biological Engineering, South China University of Technology, Guangzhou, China
[4]Department of Pathology, The First Affiliated Hospital of Nanjing Medical University, Nanjing, China
[5]Department of Pathology, Jinling Hospital, Affiliated Hospital of Medical School, Nanjing University, Nanjing, China
*Corresponding Author: Jiandong Wang. Email: jiandong_wang@nju.edu.cn
#These authors contributed equally to this work as the co-first authors

Received: 27 February 2026; Accepted: 08 May 2026; Published: 27 July 2026

ABSTRACT: Background: Rho GTPase-activating protein 40 (ARHGAP40), downregulated in various tumors, including basal cell carcinoma, has an unclear role in colorectal cancer (CRC). This study aimed to elucidate the function and clinical significance of ARHGAP40 in CRC. **Methods:** ARHGAP40 expression in CRC tissues was evaluated by immunohistochemistry and analyzed in relation to clinicopathological features and patient survival. Gain- and loss-of-function experiments were performed in CRC cell lines to assess cell proliferation, apoptosis, migration, and invasion. RNA sequencing, co-immunoprecipitation, Ras homolog gene family member A (RhoA) activation assays, and rescue experiments were conducted to explore the underlying mechanism. **Results:** ARHGAP40 expression was significantly decreased in CRC tissues and cell lines. Low ARHGAP40 expression was associated with poor differentiation ($p < 0.001$), deeper tumor invasion ($p = 0.004$), lymph node metastasis ($p < 0.001$), advanced TNM stage ($p < 0.001$), and unfavorable prognosis in patients with CRC ($p < 0.05$). Functional experiments showed that ARHGAP40 overexpression suppressed CRC cell proliferation, migration, and invasion, while promoting apoptosis, whereas ARHGAP40 knockdown exerted opposite effects. Mechanistically, ARHGAP40 interacted with RhoA and negatively regulated its activation. Moreover, restoration of RhoA activity partially reversed the effects of ARHGAP40 overexpression on CRC cell proliferation and apoptosis. **Conclusions:** ARHGAP40 is downregulated in CRC, and its loss may contribute to tumor progression, possibly through dysregulation of RhoA activity.

KEYWORDS: Rho GTPase-activating protein 40; colorectal cancer; Ras homolog gene family; member A activity

1 Introduction

A large number of people suffer from colorectal cancer (CRC), which influences the digestive system. Based on global cancer statistics from 2022, colorectal cancer has the third-highest rate of new cases and the second-highest rate of deaths [1]. Even though advancements in surgery, chemotherapy, and radiation therapy have reduced the rates of recurrence and death, multidrug resistance remains a significant problem for effective disease treatment, and the survival rates of CRC patients have not improved significantly [2,3]. To gain a deeper understanding of the progression of CRC, further research is necessary. This could lead to the identification of new therapeutic targets and diagnostic biomarkers.

As Rho homologous GTPase-activating proteins, ARHGAPs are very important for controlling the Rho family of small GTPases and their effects on many biological processes, including cell growth, adhesion, migration, and invasion [4,5]. New studies show that the ARHGAP family may also play a role in the development of several cancers. One study showed that ARHGAP1 controls the epithelial-to-mesenchymal transition (EMT) in breast cancer cells by blocking RhoA signaling [6]. Genes in the ARHGAP family have also been linked to the development of colorectal cancer in several studies, but the exact role of these genes in colorectal cancer is still not clear. The generation of a distinctive RHOGAP variant with a unique functional domain by ARHGAP8 contributes to the development of CRC [7]. The expression change of p300 by ARHGAP30 leads to the apoptosis of colorectal cancer cells, which makes the tumor suppressor protein p53 more active and acetylated [8]. Our most recent study shows that methylation significantly lowers ARHGAP40 levels in basal cell carcinoma (BCC), which suggests that it could be used as a new biomarker to tell the difference between BCC and trichoblastoma [9]. We still need to acquire more knowledge about the expression of ARHGAP40 in colorectal cancer and its role in clinical scenarios.

RhoA is a small GTPase belonging to the Rho family and stands for Ras homologue family member A. RhoA and other GTPases function as molecular switches, changing from an active state bound to GTP to an inactive state governed by GAPs [10]. The activation of RhoA is a highly important part of the reorganization of the actin cytoskeleton and exerts a considerable influence on the growth and invasion of colorectal cancer cells [11,12]. Further research needs to be conducted to figure out exactly how RhoA leads to the growth of CRC at the molecular level.

The present study aimed to explore the expression, clinical relevance, and functional role of ARHGAP40 in colorectal cancer, with a particular focus on its relationship with RhoA signaling. We hypothesized that ARHGAP40 is downregulated in CRC and that its loss promotes tumor progression, at least in part, through activation of RhoA. To address this, we evaluated ARHGAP40 expression in CRC tissues and cell lines, analyzed its clinical and prognostic significance, and investigated its biological effects in CRC cells using gain- and loss-of-function assays.

2 Materials and Methods

2.1 Patients and Samples

This study included 103 patients with CRC. All patients were recruited from Jinling Hospital, underwent surgical resection and had not received prior chemotherapy or radiotherapy. Clinical and pathological characteristics of the cohort are summarized in Table 1. Formalin-fixed, paraffin-embedded (FFPE) CRC tissues with different histological differentiation and matched adjacent non-tumorous colorectal tissues were obtained from the Department of Pathology, Jinling Hospital, and were used as archived samples for retrospective research in accordance with institutional regulations. The study protocol was reviewed and approved by the Jinling Hospital Ethics Committee (2025DZKY-051-01), which waived the requirement for informed consent due to the retrospective nature of the analysis.

Table 1: Combined characteristics of all 103 patients in the present study.

Characteristic		Cases (%)
Sex	Male	63 (61.17%)
	Female	40 (38.83%)
Age, years	≤65	54 (52.43%)
	>65	49 (47.57%)

Table 1: *Cont.*

Characteristic		Cases (%)
T stage	T1	6 (5.83%)
	T2	17 (16.50%)
	T3	24 (23.30%)
	T4	56 (54.37%)
Differention	Well/moderately differentiated	74 (71.84%)
	Poorly differentiated	29 (28.16%)
Lymph node metastases	Yes	56 (54.37%)
	No	47 (45.63%)
TNM Stage	I	17 (16.50%)
	II	30 (29.13%)
	III	51 (49.51%)
	IV	5 (4.85%)

2.2 Immunohistochemical Staining

Immunohistochemical staining was performed on 3–4 μm sections of formalin-fixed, paraffin-embedded tumor tissues according to standard procedures. The sections were deparaffinized in xylene and rehydrated through a graded ethanol series (100%, 95%, 85%, and 75%). Antigen retrieval was performed using 10 mM citrate buffer (pH 6.0). Endogenous peroxidase activity was blocked with 3% hydrogen peroxide for 10 min at room temperature, followed by blocking with 5% bovine serum albumin for 30 min. The sections were then incubated overnight at 4°C with anti-ARHGAP40 antibody (Novus Biologicals, Centennial, CO, USA, Cat. No. NBP1-94112) at a dilution of 1:1000 in 0.01 M phosphate-buffered saline (PBS, pH 7.4). Subsequently, the sections were incubated with an HRP-conjugated secondary antibody kit (PV9003, Zhongshan Golden Bridge Biotechnology, Beijing, China) at room temperature for 30 min. After washing with 0.01 M PBS, immunoreactivity was visualized using DAB working solution (Zhongshan Golden Bridge Biotechnology, Beijing, China, Cat. No. ZLI-9018) prepared according to the manufacturer's instructions, followed by hematoxylin counterstaining. Images were captured using an Olympus BX61 microscope (Olympus, Tokyo, Japan) at ×400 magnification and analyzed using Image-Pro Plus software version 6.0 (Media Cybernetics, Rockville, MD, USA). ARHGAP40 expression was classified as low (score 0–1) or high (score 2–3).

2.3 Cell Lines and Cell Culture

We get human colorectal cancer cell lines SW480, HCT116, and SW620 from American Type Culture Collection (ATCC; Manassas, VA, USA). We also get normal colonic epithelial cells NCM-460 and the human embryonic kidney epithelial cell line HEK293T from ATCC (USA). The cells were grown in high-glucose DMEM medium (Gibco, Grand Island, NY, USA) with 10% FBS (Gibco, USA) added to it. The cells were grown at 37°C with 5% CO_2. All cell lines used in this study were authenticated by STR profiling and tested negative for mycoplasma contamination.

2.4 Lentiviral Vector Infection

The ARHGAP40 overexpression plasmid was constructed by inserting the full-length ARHGAP40 coding sequence into the pLVX-IRES-puro lentiviral vector. The pLVX-IRES-puro empty vector, pLVX-IRES-puro-ARHGAP40 plasmid, and packaging plasmids psPAX2 and pMD2.G were purchased from Youbao Biological Co., Ltd. (Changsha, China). These plasmids were co-transfected into HEK293T cells using Lipofectamine 2000 reagent (Invitrogen, Carlsbad, CA, USA; Cat. No. 11668019). Viral supernatants were

collected 48 h after transfection and used to infect human CRC cell lines. Subsequently, puromycin was used for selection to establish stable ARHGAP40-overexpressing cell lines. Successful overexpression of ARHGAP40 was confirmed by RT-qPCR.

2.5 RNA Interference (siRNA)

Transient knockdown of ARHGAP40 in SW480, HCT116, and SW620 cells was conducted using siRNA (targeting sequence: siRNA-1: 5′-CUGAUUUGCUCAAAAGGUUCA-3′; siRNA-2: 5′-AGGCAAAAU UGUUUCGAAAGUGG-3), synthesized by Sangon Biotech (Shanghai, China). SW480, HCT116, and SW620 cells were transfected with small interfering RNAs (siRNAs) using Lipofectamine 2000 reagent (Invitrogen, Carlsbad, CA, USA; Cat. No. 11668019) according to the manufacturer's guidelines. The effects of RNA silencing were then verified by RT-qPCR.

2.6 Analysis of Cell Viability

SW480, HCT116, and SW620 cells in the logarithmic growth phase were put in 96-well plates so that there were 2000 cells in each well. The cells were grown in an incubator for 0, 1, 2, 3, and 4 days. Then, 10 μL of CCK-8 solution (Sangon, Shanghai, China, Cat. No. E606335) was added to each well, and then incubated at 37°C for 4 h. After that, a microplate reader (Tecan Group Ltd., Männedorf, Switzerland, M200 PRO) was used to measure the absorbance of each well at 450 nm.

2.7 Scratch Assay

SW480, HCT116, and SW620 cells were grown in a 6 cm dish until they were fully covered. At that point, a 100 μL pipette tip was used to make a scratch. The cells were washed to get rid of dirt and then grown in serum-free medium. At 0 and 12 h, pictures were taken with an Olympus IX71 microscope (Tokyo, Japan, magnification 200×), and ImageJ (version 1.53, National Institutes of Health, Bethesda, MD, USA) was used to measure the distance that cells moved. There were three analyses, and the findings shown are representative of all three.

2.8 Transwell Assay

Transwell assays were performed to evaluate cell migration and invasion. For the migration assay, 5×10^5 SW480, HCT116, and SW620 cells in serum-free medium were seeded into the upper chamber (Corning, Corning, NY, USA), while medium containing 10% FBS was added to the lower chamber. After 48 h, non-migrated cells were removed, and migrated cells were fixed with 4% paraformaldehyde and stained with 0.1% crystal violet. For the invasion assay, the upper chamber was precoated with Matrigel, and the remaining procedures were the same as those used for the migration assay. Images were captured under a phase-contrast microscope (Olympus IX71, Tokyo, Japan) at ×200 magnification, and cells were counted in three random fields per membrane.

2.9 Detection of Apoptosis by Annexin V/PI Staining

We used Annexin V/propidium iodide (PI) labelling (Sangon, Shanghai, China, Cat. No. E606336) to check for cell apoptosis in SW480, HCT116, and SW620 cells. Briefly, cells were collected, washed with cold PBS, and resuspended in 1× binding buffer, followed by staining with Annexin V-FITC and PI in the dark for 15 min. Apoptotic cells were immediately analyzed using a Beckman Coulter flow cytometer (Beckman, Brea, CA, USA), and the data were processed with FlowJo software (10.8.1).

2.10 Reverse Transcription Quantitative PCR (RT-qPCR)

To get the total RNA of SW480, HCT116, and SW620 cells, an RNA extraction kit (Cat. No. B618583) from Sangon Biotech in Shanghai, China, was used. Total RNA was reverse transcribed into cDNA using M-MuLV reverse transcriptase (Sangon Biotech, Shanghai, China, Cat. No. B600005) according to the manufacturer's instructions (42°C for 60 min, followed by 70°C for 10 min). RT-qPCR was then performed using Green-2-Go qPCR Master Mix (Sangon Biotech, Shanghai, China; Cat. No. B630004) under the following conditions: 95°C for 3 min, followed by 40 cycles of 95°C for 3 s and 60°C for 20 s. All reactions were performed in triplicate. As a standard gene, GAPDH was used. For RT-qPCR, the primers had the following sequences:

ARHGAP40: 5′-TTGGATGGAGGTGGAACAGAT-3′ (forward)
5′-GCACTGAGCGAGCATAGATG-3′ (reverse);
GAPDH: 5′-GAAGGTGAAGGTCGGAGTCA-3′ (forward)
5′-TTGAGGTCAATGAAGGGGTC-3′ (reverse).
An analysis of relative quantification was conducted using the $2^{-\Delta\Delta Ct}$ method.

2.11 RNA Sequencing

High-throughput RNA sequencing was performed to explore the potential role of ARHGAP40 in colorectal cancer progression. Total RNA was extracted from SW620 cells transfected with ARHGAP40 siRNA or negative control siRNA using TRIzol reagent (Sangon Biotech, Shanghai, China). One biological replicate was included for each group (n = 1). RNA quality was assessed prior to library construction, and only samples with an RNA integrity number (RIN) $\geq$ 7.0 were used for sequencing. The sequencing work was conducted by Novogene Biotech Co., Ltd. (Beijing, China). Sequencing libraries were prepared using the NEBNext Ultra™ RNA Library Prep Kit for Illumina (NEB, Ipswich, MA, USA) according to the manufacturer's instructions, and library quality was evaluated using an Agilent Bioanalyzer 2100 (Agilent Technologies, Santa Clara, CA, USA). The libraries were sequenced on the Illumina NovaSeq 6000 platform (Illumina, San Diego, CA, USA). Clean reads were aligned to the human reference genome GRCh38. Differential expression analysis was performed using the 'DESeq2' package (1.46.0) in R (4.4.1), and genes with $|\log2FC| > 1$ and $p_{adj} < 0.05$ were considered significantly differentially expressed. Functional enrichment analyses, including KEGG and Reactome pathway analyses, were subsequently performed based on the differentially expressed genes. Volcano plots were generated using the 'EnhancedVolcano' (1.18.0) package in R. The database sources were as follows: KEGG (https://www.genome.jp/kegg/pathway.html) and Reactome (https://reactome.org/).

2.12 Protein–Protein Interaction (PPI) Network Analysis

In order to analyze differentially expressed genes (DEGs), a protein–protein interaction (PPI) network analysis was performed using the STRING database (http://string-db.org/). The PPI network data files were visualized using the Cytoscape software (3.9.1), and key genes were identified.

2.13 Western Blot and Immunoprecipitation (IP) Analyses

Western blotting was performed using standard procedures. Briefly, SW480, HCT116, and SW620 cells were lysed in RIPA buffer containing protease inhibitors (Beyotime Biotechnology, Shanghai, China; Cat. No. P0013B) on ice for 30 min, and the lysates were centrifuged to collect the supernatants. Protein concentration was determined using a BCA Protein Assay Kit (Beyotime Biotechnology, Shanghai, China; Cat. No. P0010). Equal amounts of protein (100 μg) were separated by 4%–20% SDS-PAGE and transferred

onto PVDF membranes. After blocking with 5% nonfat milk, the membranes were incubated overnight at 4°C with primary antibodies against GAPDH (Cell Signaling Technology, Danvers, MA, USA; Cat. No. 5174; diluted 1:1000) and RhoA (Abcam, Cambridge, UK; Cat. No. ab187027; diluted 1:1000), followed by incubation with an HRP-conjugated secondary antibody (Beyotime Biotechnology, Shanghai, China; Cat. No. A0208; diluted 1:5000). Protein bands were visualized using an enhanced chemiluminescence reagent (ACE Biotechnology, Xiangtan, Hunan, China; Cat. No. BK0041) and imaged with a Tanon 5200 chemiluminescent imaging system (Tanon Science & Technology Co., Ltd., Shanghai, China).

Co-immunoprecipitation (co-IP) was performed to examine the interaction between ARHGAP40 and RhoA. SW480, HCT116, and SW620 cells were lysed in ice-cold lysis buffer, and the lysates were clarified by centrifugation. A portion of each lysate was reserved as the input control. For each IP reaction, 500–1000 μg of total protein was used. rProtein A/G magnetic beads (ACE Biotechnology, Cat. No. BK0004) were equilibrated and pre-washed with 1× Lysis/Wash Buffer (Enhanced) according to the manufacturer's instructions. Briefly, 20 μL of magnetic beads were incubated with 1 μg of anti-FLAG (DYKDDDDK) antibody (ACE Biotechnology, Cat. No. MP5101) or 1 μg of mouse IgG isotype control (Cell Signaling Technology, Cat. No. 5415) with rotation for 1 h at room temperature. The antibody-bead complexes were then washed with 1× Lysis/Wash Buffer (Enhanced), followed by incubation with the cell lysates at 4°C overnight with rotation. After immunoprecipitation, the beads were washed three times with 1× Lysis/Wash Buffer (Enhanced) under gentle mixing. The bound immune complexes were finally eluted in SDS sample buffer and analyzed by Western blotting.

2.14 Detection of RhoA Activity

RhoA activity was assessed using a RhoA Activation Assay Kit (NewEast Biosciences, Wuhan, China; Cat. No. 80601) according to the manufacturer's instructions. Briefly, SW480, HCT116, and SW620 cells were washed twice with ice-cold PBS and lysed in 1× Assay/Lysis Buffer (NewEast Biosciences, Wuhan, China; Cat. No. 30302) supplemented with protease inhibitors on ice for 10–20 min. The lysates were then collected and clarified by centrifugation at 12,000× *g* for 10 min at 4°C. The supernatants were collected and kept on ice for immediate use. For each pull-down reaction, 0.5–1 mL of cell lysate containing approximately 1 mg of total protein was adjusted to a final volume of 1 mL with 1× Assay/Lysis Buffer, followed by incubation with 1 μL anti-RhoA-GTP mouse monoclonal antibody (NewEast Biosciences, Wuhan, China; Cat. No. 26904) and 20 μL resuspended Protein A/G agarose bead slurry (NewEast Biosciences, Wuhan, China; Cat. No. 30301) at 4°C for 1 hwith gentle agitation. The beads were then pelleted, washed three times with 0.5 mL 1× Assay/Lysis Buffer, and finally resuspended in 20 μL 2× reducing SDS-PAGE sample buffer. After boiling for 5 min, the samples were centrifuged briefly and subjected to western blotting using an anti-RhoA rabbit polyclonal antibody (NewEast Biosciences, Wuhan, China; Cat. No. 80601; Cat. No. 21017, diluted 1:500).

2.15 RhoA Rescue Experiments

To verify whether RhoA mediates the biological effects of ARHGAP40 in CRC cells, rescue experiments were performed by co-transfecting cells with an ARHGAP40 overexpression plasmid and a constitutively active RhoA (RhoA-Q63L) plasmid. Cells were assigned to three groups: vector, ARHGAP40, and ARHGAP40 + RhoA-Q63L. Forty-eight hours after transfection, cell proliferation and apoptosis were evaluated by CCK-8 assay and flow cytometry, respectively.

2.16 Survival Analysis

The publicly available datasets GSE17537, GSE14385, GSE12945, GSE17536, and GSE14333 with survival information were obtained from the Gene Expression Omnibus (GEO) database (https://www.ncbi.nlm.nih.gov/geo/) and analyzed using the PrognoScan database (http://www.prognoscan.org/) to evaluate the associations between ARHGAP40 expression and OS or DFS in CRC patients. When the survival curves crossed, indicating potential non-proportional hazards, landmark analysis was additionally performed [13]. A total of 103 colorectal cancer patients were enrolled in this study, among whom 92 had complete follow-up and survival information. These 92 patients were included in the survival analysis. Kaplan–Meier survival curves were generated, and differences between groups were assessed using the log-rank test.

2.17 Statistical Analysis

Statistical analyses were performed using IBM SPSS Statistics version 24.0 (IBM Corp., Armonk, NY, USA). Continuous variables are presented as the mean ± standard deviation (SD) and were compared between two groups using Student's *t*-test. ARHGAP40 expression was classified according to the immunohistochemical staining score, with scores of 0–1 defined as low expression and scores of 2–3 defined as high expression. Associations between ARHGAP40 expression and clinicopathological characteristics were analyzed using the Chi-square test. Among the 103 enrolled patients, 92 with complete follow-up and survival data were included in the survival analysis. Overall survival was analyzed using the Kaplan-Meier method and compared using the log-rank test. Landmark analysis was additionally performed when the survival curves crossed. All tests were two-sided, and $p < 0.05$ was considered statistically significant.

3 Results

3.1 ARHGAP40 Is Downregulated in CRC Tissues and Cells

To investigate the role of ARHGAP40 in colorectal cancer (CRC), we first performed immunohistochemical (IHC) staining to assess ARHGAP40 expression in CRC tissues. As shown in Fig. 1A and summarized in Table 2, ARHGAP40 expression was significantly reduced in CRC tumor tissues compared to adjacent non-tumorous tissues (Fig. 1A; Table 2, $p < 0.001$). Furthermore, we evaluated ARHGAP40 mRNA levels in colorectal cancer cell lines and the normal colorectal epithelial cell line NCM-460. The results indicated that ARHGAP40 expression was markedly lower in colorectal cancer cells than in NCM-460 cells (Fig. 1B). Collectively, these findings demonstrate that ARHGAP40 is expressed at low levels in both colorectal cancer cells and tumor tissues.

Table 2: Expression of ARHGAP40 in CRC tumors and adjacent normal tissues.

ARHGAP40 Expression	Tumor Tissue		Adjacent Normal Tissue		*p* Value
	Cases	Percentage	Cases	Percentage	
Low	50	48.54%	27	26.21%	<0.001***
High	53	51.46%	76	73.79%	

Note: $p < 0.05$ was considered statistically significant, ***, $p < 0.001$.

3.2 Correlations between ARHGAP40 Expression Levels and Clinicopathological Parameters in CRC Patients

We further analyzed the association between ARHGAP40 expression and clinicopathological characteristics of CRC patients. Chi-square test results demonstrated that reduced ARHGAP40 expression was significantly correlated with increased lymph node metastasis, greater tumor invasion depth ($p = 0.004$),

poorer tumor differentiation ($p < 0.001$), and higher TNM stage ($p < 0.001$) (Table 3). Additionally, ARHGAP40 expression showed significant associations with patients' age ($p = 0.014$) and sex ($p = 0.008$) (Table 3). Collectively, these findings indicate that reduced ARHGAP40 expression is associated with unfavorable clinicopathological features and may reflect a more aggressive CRC phenotype.

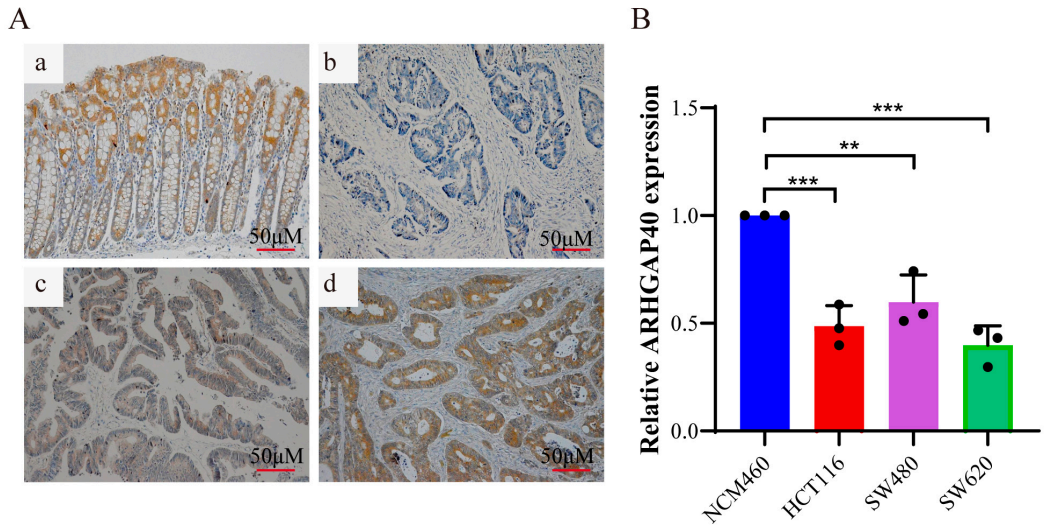

Figure 1: Low expression of ARHGAP40 was observed in CRC tissue samples and CRC cell lines. (**A**) Representative immunohistochemical staining results of ARHGAP40 in colorectal cancer (CRC) tissues of different differentiation degrees and adjacent non-tumor tissues (magnification, 400×). (**a**) Normal human colon tissues; (**b**) poorly differentiated CRC; (**c**) moderately differentiated CRC; (**d**) well-differentiated CRC. (**B**) Expression profile of the ARHGAP40 gene in normal intestinal epithelial cell line and colorectal cancer cell lines measured using RT-qPCR (Colors indicate different cell lines: blue, NCM460; red, HCT116; purple, SW480; and green, SW620.). **, $p < 0.01$, ***, $p < 0.001$.

Table 3: Association between ARHGAP40 expression and the clinicopathological features of CRC.

Characteristics		ARHGAP40 Expression		χ^2	*p*-Value
		Low	High		
Sex	Male	24	39	7.090	0.008**
	Female	26	14		
Age	≤65	20	34	6.017	0.014*
	>65	30	19		
Invasion Depth	T1/T2	5	18	8.518	0.004**
	T3/T4	45	35		
Differentiation	High/Moderate	26	48	18.971	<0.001***
	Poorly	24	5		
Lymph node metastasis	No	4	43	55.464	<0.001***
	Yes	46	10		
TNM Stage	I/II	5	42	49.725	<0.001***
	III/IV	45	11		

Note: $p < 0.05$ was considered statistically significant; *, $p < 0.05$, **, $p < 0.01$, ***, $p < 0.001$. The χ^2 test was performed.

3.3 ARHGAP40 Promotes Apoptosis and Inhibits Proliferation in Colorectal Cancer Cells

Given that reduced ARHGAP40 expression is closely associated with disease progression in colorectal cancer, we further investigated the functional role of ARHGAP40 in CRC cells. We manipulated ARHGAP40 expression in SW480, SW620, and HCT116 cell lines by transfecting them with either an ARHGAP40 overexpression plasmid or ARHGAP40-targeted siRNA. RT-qPCR analysis confirmed efficient overexpression and knockdown of ARHGAP40 (Fig. 2A,B). CCK-8 assays demonstrated that upregulation of ARHGAP40 significantly decreased cell viability across all three CRC cell lines (Fig. 2C), whereas silencing ARHGAP40 resulted in enhanced cell proliferation (Fig. 2D). Additionally, flow cytometry analysis revealed that ARHGAP40 overexpression markedly increased apoptosis in CRC cells (Fig. 2E), while ARHGAP40 knockdown substantially reduced cell apoptosis compared with the control group (Fig. 2F). Similar results were obtained using a second independent siRNA targeting ARHGAP40, which also promoted CRC cell proliferation and inhibited apoptosis (Supplementary Fig. S1A–C). Collectively, these findings suggest that ARHGAP40 suppresses CRC cell proliferation and promotes apoptotic cell death.

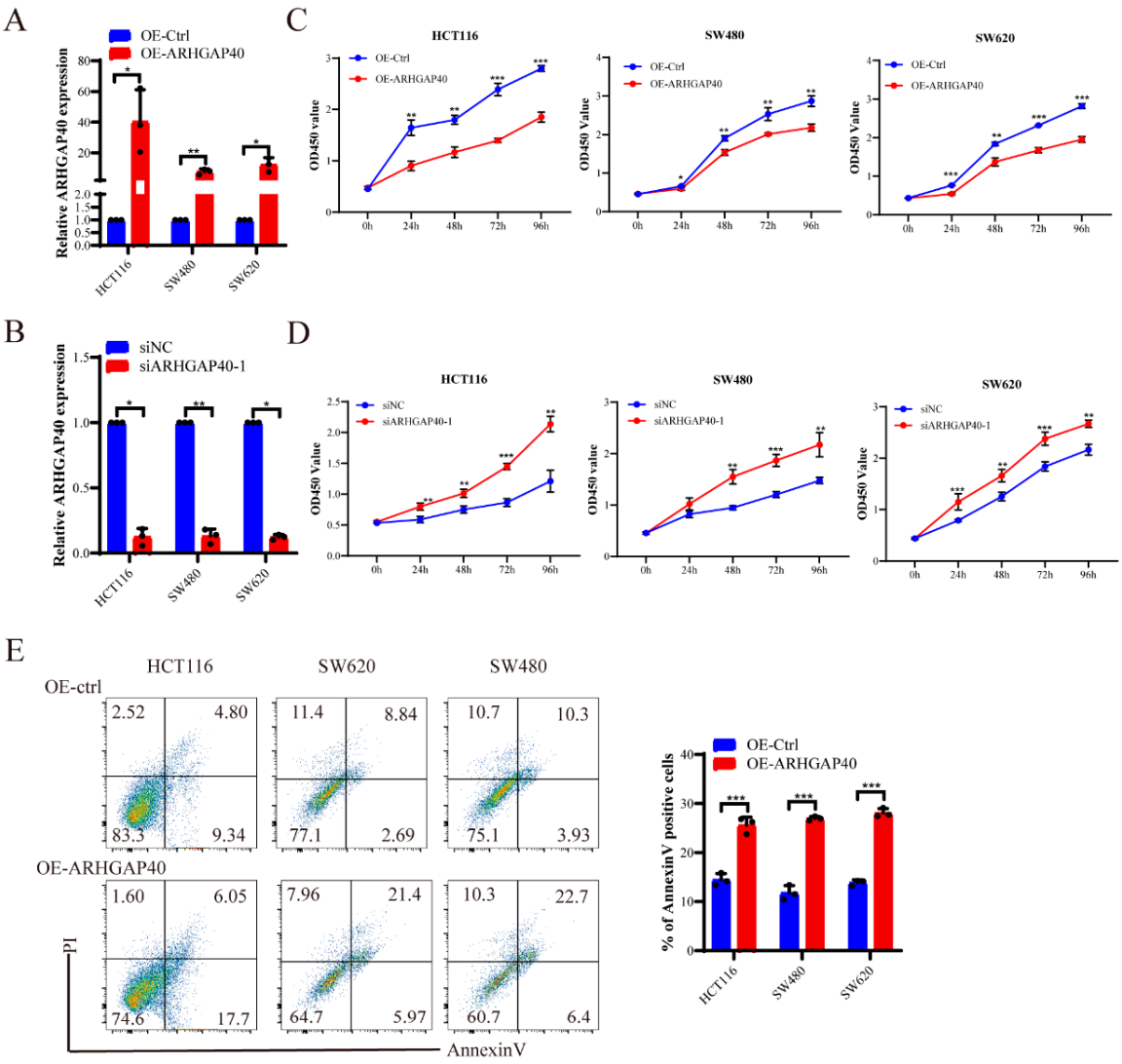

Figure 2: *Cont.*

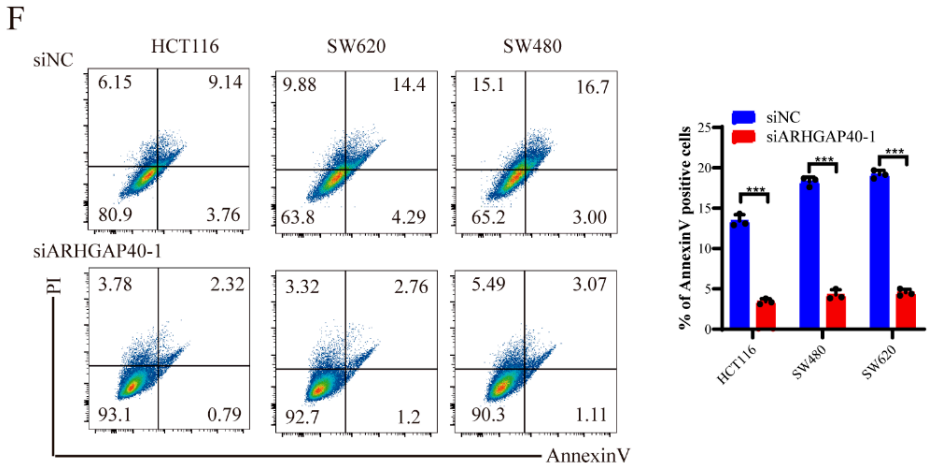

Figure 2: ARHGAP40 modulates cell viability and apoptosis *in vitro*. (**A**) ARHGAP40 mRNA expression following overexpression, quantified by RT–qPCR. (**B**) Relative ARHGAP40 mRNA expression in cells transfected with si-ARHGAP40-1, as determined by RT-qPCR. (**C**) Cell viability was assessed by the CCK-8 assay after ARHGAP40 overexpression. (**D**) Effects of si-ARHGAP40-1 on cell viability, as assessed by CCK-8. (**E**) Apoptotic rates of ARHGAP40-overexpressing cells were determined by flow cytometry. Blue and red bars represent OE-Ctrl and OE-ARHGAP40 groups, respectively. (**F**) Effects of si-ARHGAP40-1 on apoptosis, as determined by flow cytometry. Blue and red bars represent siNC and siARHGAP40-1 groups, respectively. *, $p < 0.05$; **, $p < 0.01$; ***, $p < 0.001$.

3.4 ARHGAP40 Inhibits the Migration and Invasion of Colorectal Cancer Cells

We employed scratch and Transwell assays to assess the impact of ARHGAP40 on the migratory and invasive abilities of CRC cells. The scratch assay demonstrated that cells transfected with the ARHGAP40 overexpression vector exhibited significantly slower wound closure compared to cells transfected with the control vector (Fig. 3A). Similarly, Transwell migration assays revealed a marked reduction in cell migration rates in ARHGAP40-overexpressing cells relative to negative controls (Fig. 3B). Consistent results were observed in Matrigel invasion assays, where ARHGAP40 overexpression significantly impaired the invasive capacity of CRC cells (Fig. 3B).

Conversely, knockdown of ARHGAP40 led to enhanced migration and invasion of colorectal cancer cells, as demonstrated by both scratch and Transwell invasion assays (Fig. 3C,D). These findings suggest that ARHGAP40 may inhibit the migratory and invasive potentials of CRC cells.

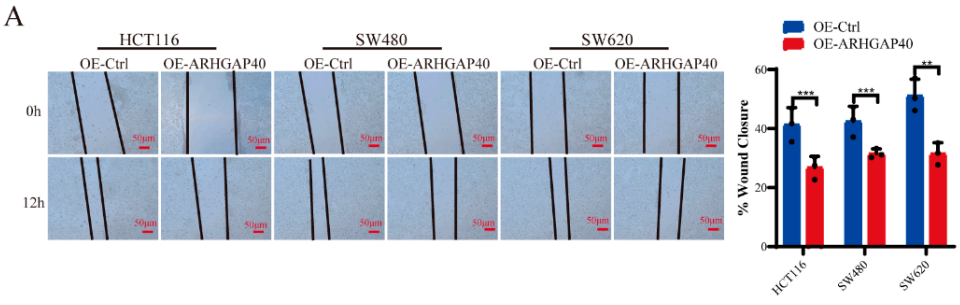

Figure 3: *Cont.*

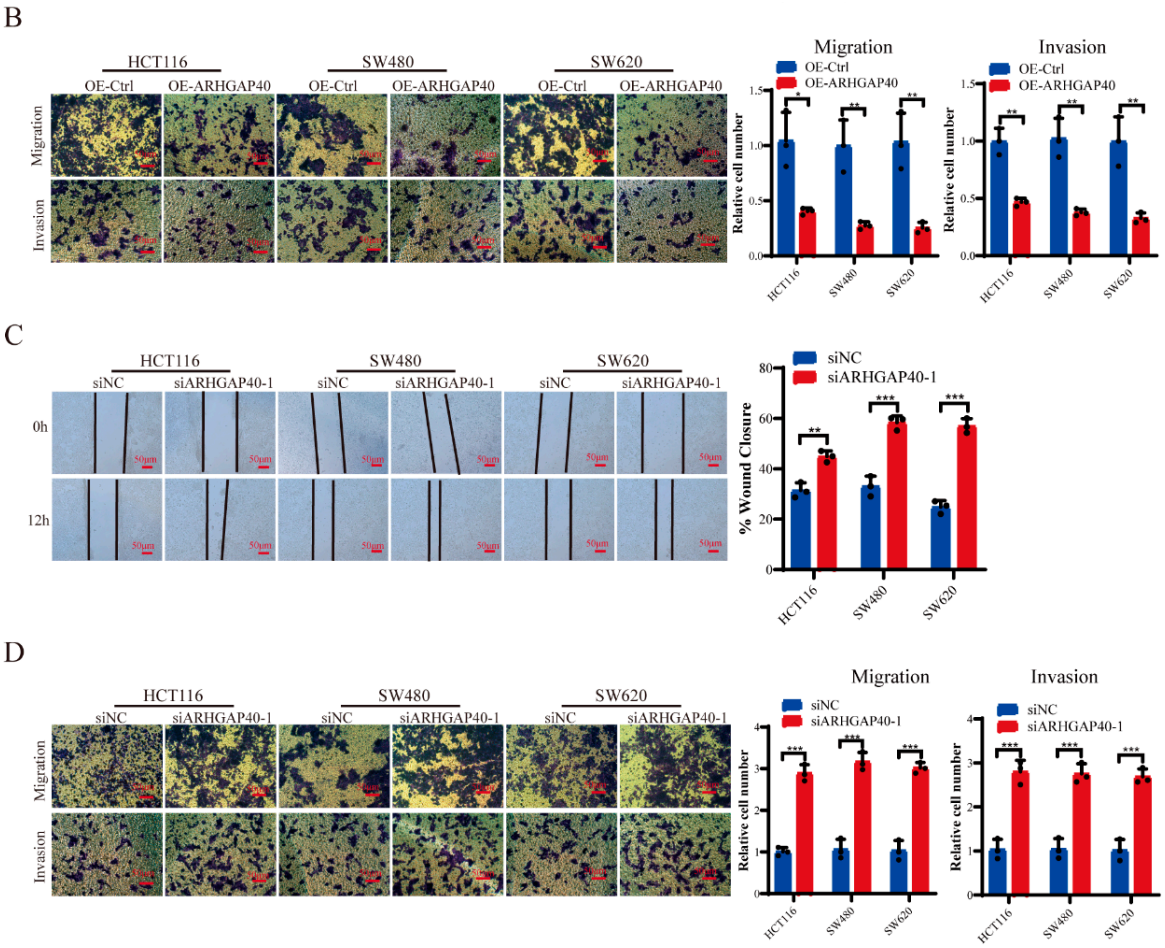

Figure 3: ARHGAP40 regulates migratory and invasive capacities of colorectal cancer cells. (**A**) Representative images and quantitative analysis of scratch assays in ARHGAP40-overexpressing and control CRC cells (200×). (**B**) Representative images and quantification of Transwell migration and invasion assays in ARHGAP40-overexpressing and control CRC cells (200×). (**C**) Representative images and quantitative analysis of scratch assays assays after si-ARHGAP40-1 transfection in CRC 200×). (**D**) Representative images and quantitative analysis of Transwell migration and invasion assays after si-ARHGAP40-1 transfection in CRC cells (200×). *, $p < 0.05$; **, $p < 0.01$; ***, $p < 0.001$.

3.5 Low ARHGAP40 Expression Is Associated with the Prognosis of CRC

Our previous findings demonstrated that ARHGAP40 expression is markedly reduced in tumor tissues from patients with colorectal cancer (CRC). To further explore the prognostic value of ARHGAP40, we analyzed data from the GEO database, examining its association with survival outcomes in CRC. Five independent datasets were utilized: GSE17537 (177 samples), GSE143985 (91 samples), GSE17536 (56 samples), GSE12945 (62 samples), and GSE14333 (290 samples), encompassing CRC cases at various clinical stages.

Analysis revealed that lower ARHGAP40 expression was significantly associated with reduced overall survival (OS) in both the GSE17537 and GSE143985 cohorts (GSE17537, HR = 0.61, 95% CI = 0.17–2.21, Cox $p = 0.014$; GSE143985, HR = 0.2892, 95% CI = 0.1046–0.8000, Cox $p = 0.0169$; Fig. 4A). Furthermore, in the GSE17536, GSE12945, and GSE14333 cohorts, decreased ARHGAP40 expression was strongly correlated with shorter disease-free survival (DFS) (GSE17536, HR = 0.4169, 95% CI = 0.2076–0.8375, Cox $p = 0.0140$; GSE14333, HR = 0.3239, 95% CI = 0.1342–0.7817, Cox $p = 0.0121$; Fig. 4B). In addition, Kaplan-Meier survival

analysis of 92 CRC patients from our own cohort showed that patients with low ARHGAP40 protein expression had significantly poorer survival than those with high ARHGAP40 expression (p = 0.0274; Fig. 4C). Collectively, these results indicate that the downregulation of ARHGAP40 in CRC is associated with poorer prognosis.

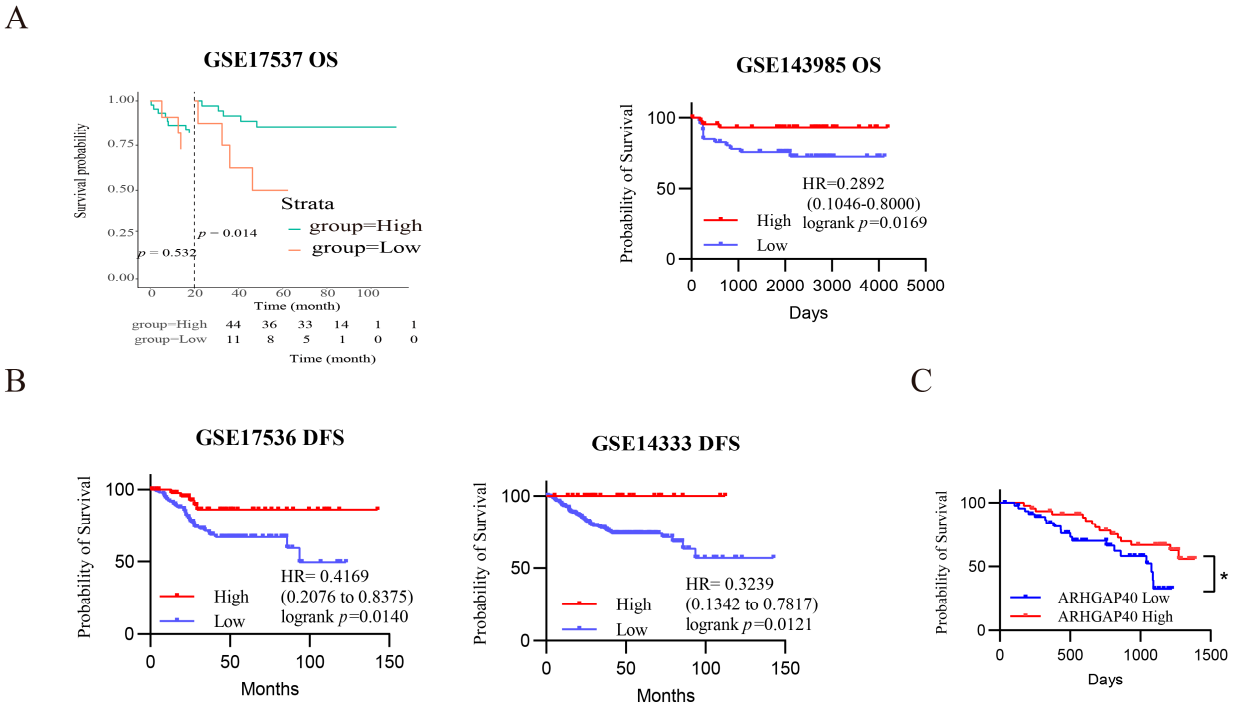

Figure 4: Survival analysis of ARHGAP40 mRNA expression according to the GEO databases. (**A**) Kaplan–Meier survival analysis of ARHGAP40 levels with OS in CRC patients in the GEO database. (**B**) Kaplan–Meier survival analysis of ARHGAP40 levels with DFS in CRC patients in the GEO database. (**C**) Kaplan–Meier survival analysis of ARHGAP40 expression and overall survival in CRC patients from our institutional cohort. *, $p < 0.05$.

3.6 ARHGAP40 Functions by Regulating the Activity of RhoA in CRC Cells

ARHGAP40 exerts its effects in CRC cells primarily by regulating RhoA activity. To elucidate the underlying mechanisms and signaling pathways influenced by ARHGAP40, we performed RNA sequencing on ARHGAP40-knockdown and control CRC cells. This analysis identified 2212 differentially expressed genes (|fold change| $\geq$ 1 and $p < 0.05$) upon ARHGAP40 depletion, with 1130 genes significantly downregulated and 1082 genes significantly upregulated (Fig. 5A). KEGG enrichment analysis revealed that the upregulated genes were predominantly involved in the HIF-1 signaling pathway and glycolytic processes (Fig. 5B). Utilizing the Reactome database, we found that ARHGAP40 was associated with multiple signaling cascades, including Rho GTPase signaling, Rho GTPase effectors, receptor tyrosine kinases, WNT signaling, and GPCR downstream signaling (Fig. 5C).

Further protein–protein interaction (PPI) analysis using the STRING database suggested that ARHGAP40 interacts with members of the Rho-GTPase family, notably RhoA and CDC42 (Fig. 5D). Other ARHGAP family proteins, such as ARHGAP28, ARHGAP26, and ARHGAP18, have been reported to inactivate RhoA [14,15]. Notably, RhoA overexpression is associated with increased invasion, unfavorable prognosis, and chemotherapy resistance in CRC patients [14–16].

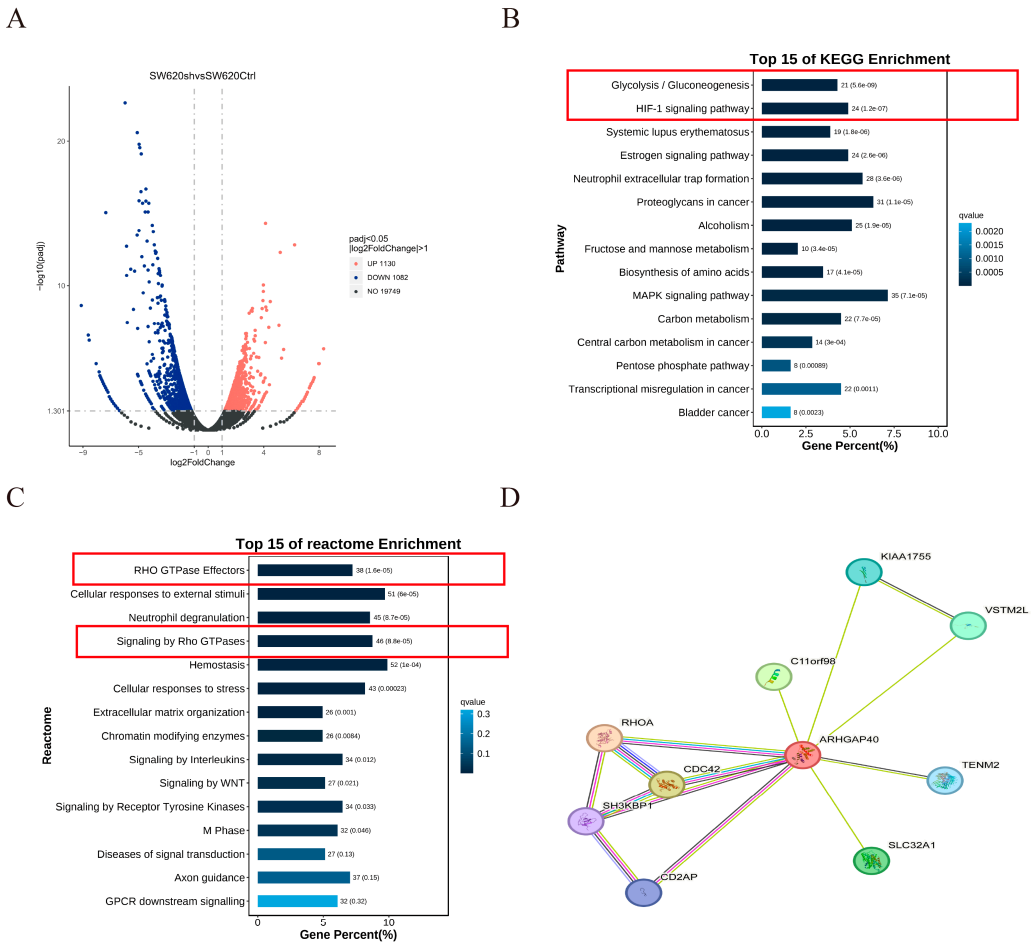

Figure 5: Pathway enrichment analysis of RNA-seq expression profiling in ARHGAP40 knockdown CRC cells. (**A**) Volcano plot displaying differential gene expression by RNA-seq in siNC versus siARHGAP40 CRC cells. (**B**) Enrichment results of the KEGG signaling pathway in DEGs revealed by RNA-seq. (**C**) The results of Reactome pathway enrichment analysis after RNA sequencing (RNA-seq). (**D**) The correlation of ARHGAP40 and other proteins is analyzed in the STRING database.

Based on these insights, we hypothesized that ARHGAP40 could directly bind to RhoA and modulate its function in CRC cells. To test this, we performed co-immunoprecipitation (co-IP) assays following transfection with Flag-ARHGAP40 or a Flag-empty vector. The results confirmed a direct interaction between ARHGAP40 and RhoA (Fig. 6A). Next, we assessed RhoA activity in CRC cell lines treated with either ARHGAP40 siRNA or control siRNA. Pull-down assays using RhoA-binding domain beads captured the active, GTP-bound RhoA, which was then quantified by Western blotting. As shown in Fig. 6B,C, ARHGAP40 overexpression significantly inhibited RhoA activation, whereas ARHGAP40 knockdown markedly increased RhoA activation. The original Western blot images are provided in Supplementary Fig. S2A–C. To further verify whether RhoA activation is involved in ARHGAP40-mediated biological effects, rescue experiments were performed using constitutively active RhoA (RhoA-Q63L). As shown in Fig. 6D,E, the inhibitory effect of ARHGAP40 overexpression on cell proliferation and its promoting effect on apoptosis were partially reversed by RhoA-Q63L co-transfection, indicating that RhoA is involved in mediating the function of ARHGAP40 in CRC cells. These findings suggest that ARHGAP40 may inhibit CRC progression by binding to and modulating RhoA activity.

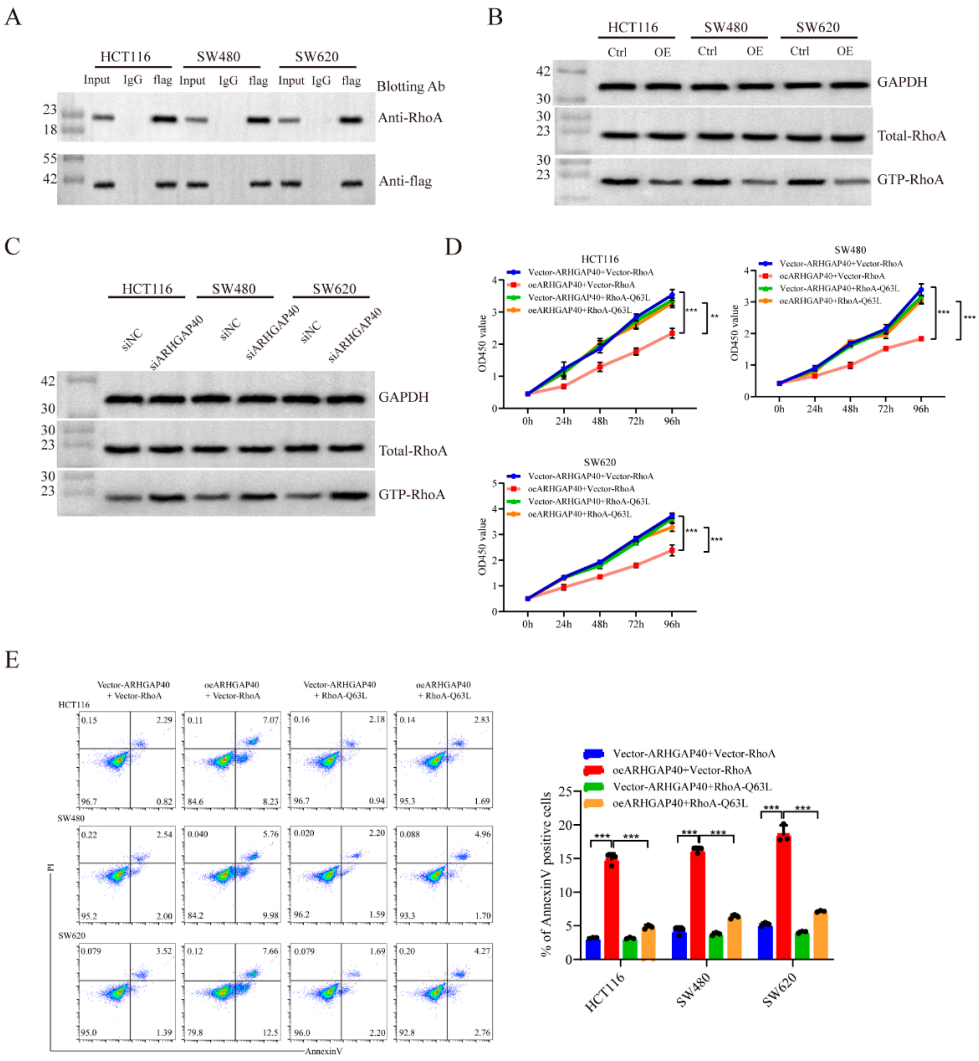

Figure 6: Interactions between ARHGAP40 and RhoA and the effect of ARHGAP40 on RhoA activity. (**A**) Co-immunoprecipitation (co-IP) assays for the interaction between ARHGAP40 and RhoA. (**B**) RhoA activation assay showing decreased RhoA activity in ARHGAP40-overexpressing CRC cells. (**C**) RhoA activation assay showing enhanced RhoA activity in ARHGAP40 knockdown CRC cells. (**D**) Rescue experiment showing the effect of RhoA-Q63L on cell viability in ARHGAP40-overexpressing CRC cells, as assessed by CCK-8 assay. (**E**) Rescue experiment showing the effect of RhoA-Q63L on apoptosis in ARHGAP40-overexpressing CRC cells, as determined by flow cytometry. **, $p < 0.01$; ***, $p < 0.001$.

4 Discussion

Despite significant advances in the diagnosis and treatment of colorectal cancer, many patients continue to experience poor prognoses due to the risk of tumor recurrence or metastasis [17]. Further research is required to gain a deeper understanding of the mechanisms underlying cancer initiation and to identify reliable biomarkers for the diagnosis of colorectal cancer. The primary objective of this study is to elucidate the role of ARHGAP40 in the progression and metastasis of colorectal cancer. Through the use of clinical specimens and *in vitro* cellular experiments, we demonstrate that ARHGAP40 suppresses tumor growth and interacts with the RhoA signaling pathway. These findings not only enhance our understanding of

the molecular mechanisms involved in colorectal cancer but also suggest that ARHGAP40 may serve as a potential therapeutic target for CRC.

The ARHGAP gene family encodes at least 32 RhoGAP proteins, which participate in a wide range of biological processes, including neuronal development, cell division, migration, angiogenesis, and tumor suppression [6,18,19]. In recent years, increasing attention has been paid to the role of ARHGAP family genes in tumorigenesis and tumor progression. For instance, ARHGAP10/GPX4 has been shown to induce ferroptosis in ovarian cancer cells and inhibit tumor growth, findings that are consistent with clinical observations [20]. Similarly, ARHGAP24 has been implicated in the proliferation and metastasis of breast cancer cells, as well as in the pathogenesis of renal cell carcinoma (RCC) and hepatocellular carcinoma (HCC) [21,22].

Recent studies have also reported associations between ARHGAP family genes and colorectal cancer (CRC). For example, the RhoGAP6 isoform 1 variant has been identified as a potential biomarker for CRC progression [23]. In addition, elevated expression of ARHGAP8 has been observed in colorectal tumor tissues, where it regulates CRC cell activity through the ARHGAP1/CDC42GAP/p50RHOGAP pathway [7,24]. Furthermore, ARHGAP4 expression is significantly increased in CRC patients and is associated with poorer prognosis [25].

To date, the role of ARHGAP40 in tumors, particularly in colorectal cancer (CRC), remains largely unexplored. To the best of our knowledge, the present study provides novel evidence supporting a tumor-suppressive role for ARHGAP40 and its potential value as a biomarker in CRC. Our findings revealed that ARHGAP40 expression is significantly reduced in both colorectal cancer cells and tissues compared to their normal counterparts. Moreover, ARHGAP40 mRNA levels were strongly associated with key clinicopathological features of CRC, including invasion depth, tumor differentiation, lymph node metastasis, and TNM stage. Mechanistic investigations further showed that ARHGAP40 suppression enhances CRC cell proliferation and inhibits apoptosis, whereas its activation exerts the opposite effects. Collectively, these results highlight the unique and important role of ARHGAP40 in regulating CRC growth and progression.

Metastasis, characterized by its selective nature, is a leading cause of cancer-related mortality [26]. In colorectal cancer, the elevated death rates are largely attributed to the dissemination of malignant cells from the primary tumor to distant sites [27]. However, the underlying mechanisms driving CRC metastasis remain incompletely understood. Previous studies have demonstrated that the ARHGAP gene family can influence tumor metastasis by regulating RhoA or other members of the Rho family [4]. Consistent with findings for other ARHGAP proteins, our study revealed that downregulation of ARHGAP40 significantly enhances the migratory and invasive abilities of colorectal cancer cells, whereas overexpression of ARHGAP40 yields the opposite effects. These results indicate that ARHGAP40 may play a crucial role in suppressing CRC cell metastasis *in vitro*, potentially through modulation of Rho GTPase signaling pathways.

Rho family proteins dynamically alternate between an active GTP-bound state and an inactive GDP-bound state. Members of the ARHGAP family regulate this transition by stimulating the intrinsic GTPase activity of Rho GTPases, thereby promoting their conversion to the inactive GDP-bound form [4,28]. RhoA, a key member of the Rho GTPase family, has been implicated in multiple malignant phenotypes, including proliferation, migration, invasion, and cytoskeletal remodeling. However, its role in CRC appears to be context-dependent rather than uniformly oncogenic. Previous studies have shown that high RhoA expression is associated with lymph node and vascular invasion as well as poorer postoperative survival in CRC patients, and more recent work has further supported a pro-tumorigenic role of the RhoA/ROCK axis in CRC growth, migration, and invasion [29]. In contrast, Rodrigues et al. reported that RHOA inactivation promoted CRC progression and metastasis, at least in part through redistribution of β-catenin from the

cell membrane to the nucleus and subsequent activation of Wnt/β-catenin signaling [30]. Therefore, the biological function of RhoA in CRC is likely determined by the specific molecular and cellular context. ARHGAP40, as a regulator of the RhoA pathway, may not simply function as an inhibitor of RhoA, but rather as a dynamic modulator of its activity. Thus, our findings are not necessarily inconsistent with previous reports, but instead further support a complex and context-dependent role of the ARHGAP40-RhoA axis in CRC progression. This interpretation is also consistent with the heterogeneous roles reported for other ARHGAP family members in CRC, with ARHGAP15 and ARHGAP24 showing tumor-suppressive effects, whereas ARHGAP4 has been reported to promote colon cancer metastasis [31,32]. Consistent with this notion, our RNA-seq data showed enhanced Rho GTPase signaling after ARHGAP40 loss, and STRING analysis suggested a potential interaction between ARHGAP40 and RhoA, indicating that ARHGAP40 may exert its biological effects, at least in part, through regulation of the RhoA pathway.

Rho GTPases play a pivotal role in the regulation of cellular signaling pathways. These molecules cycle between an active, GTP-bound state and an inactive, GDP-bound state [33]. Upon activation, Rho GTPases engage with a variety of downstream effectors, thereby influencing their activities and subcellular localization [34]. The dynamic regulation of Rho GTPase activity is orchestrated by the opposing actions of guanine nucleotide exchange factors (GEFs), which promote activation, and GTPase-activating proteins (GAPs), which facilitate inactivation [35]. Several members of the ARHGAP family, such as ARHGAP5, ARHGAP10, and ARHGAP28, have been reported to promote the intracellular accumulation of RhoA in cancer cells [36–38]. Therefore, in this study, we examined whether ARHGAP40 could function as an effective GAP for RhoA in colorectal cancer cells.

5 Limitations

This study has several limitations. First, the RNA-seq analysis was performed without biological replicates, and therefore the differential expression and pathway enrichment results should be interpreted with caution and considered exploratory. Second, some of the conclusions drawn require further validation through *in vivo* experiments. Second, additional studies are needed to confirm the relationship between ARHGAP40 and RhoA and to elucidate the underlying mechanisms. Finally, the potential interactions between ARHGAP40 and other members of the Rho family proteins warrant further investigation.

6 Conclusions

In conclusion, our research demonstrates that ARHGAP40, functioning as a tumor suppressor, is expressed at low levels in colorectal cancer and is involved in regulating cell proliferation, metastasis, and viability. Importantly, our findings indicate that ARHGAP40 may function in a tumor-suppressive manner in colorectal cancer by negatively regulating RhoA. Collectively, these results suggest that the ARHGAP40/RhoA axis may respresent a potential target for further therapeutic investigation in colorectal cancer.

Acknowledgement: We express our gratitude to Prof. Junhua Wu of the Medical School of Nanjing University for his immensely valuable guidance and assistance throughout the duration of this study. In addition, we extend our appreciation to colleagues from Guangzhou Huayin Medical Laboratory Center, including Zhihui Quan, Mingming Huang, and Jiewei Mao, for their technical support and engaging discussions. The authors gratefully acknowledge the support provided by the Guangzhou Postdoctoral Innovation Practice Base Project of Guangzhou Huayin Medical Laboratory Center Co., Ltd.

Funding Statement: The authors received no specific funding for this study.

Author Contributions: Bin Lian: Conception and design, Collection and assembly of data, Manuscript writing, Final approval of manuscript. Na You: Conception and design, Data analysis and interpretation, Manuscript writing, Final approval of manuscript. Jingyu Wang: Collection and assembly of data, Manuscript writing, Final approval of manuscript. Cong Wang: Collection and assembly of data, Manuscript writing, Final approval of manuscript. Yunjie Wen: Manuscript writing, Final approval of manuscript. Jiandong Wang: Provision of study materials or patients, Data analysis and interpretation, Manuscript writing, Final approval of manuscript. All authors reviewed and approved the final version of the manuscript.

Availability of Data and Materials: The datasets produced and inspected in the present study can be retrieved from the corresponding author [Jiandong Wang] upon request.

Ethics Approval: The study protocol was reviewed and approved by the Jinling Hospital Ethics Committee (2025DZKY-051-01), which waived the requirement for informed consent due to the retrospective nature of the analysis.

Conflicts of Interest: Bin Lian and Na You are full-time employees of Guangzhou Huayin Medical Laboratory Center Co, Ltd., which also provided funding for this study. The authors affirm that they have no additional financial or personal conflicts of interest that could have influenced the work reported in this manuscript. The authors have disclosed that they have no conflicts of interest.

Supplementary Materials: The supplementary material is available online at https://www.techscience.com/doi/10.32604/biocell.2026.081166/s1. Supplementary Fig. S1: Validation and functional effects of si-ARHGAP40-2 in CRC cells. (A) ARHGAP40 mRNA expression after si-ARHGAP40-2 transfection. (B) Cell viability after si-ARHGAP40-2 transfection. (C) Apoptosis after si-ARHGAP40-2 transfection. *, $p < 0.05$; **, $p < 0.01$; ***, $p < 0.001$. Supplementary Fig. S2: Original Western Blot images of the Western Blots for Fig. 6A–C showing the bands with molecular weight markers.

References

1. Bray F, Laversanne M, Sung H, Ferlay J, Siegel RL, Soerjomataram I, et al. Global cancer statistics 2022: GLOBOCAN estimates of incidence and mortality worldwide for 36 cancers in 185 countries. CA Cancer J Clin. 2024;74(3):229–63. [CrossRef].
2. Chen Z, He L, Zhao L, Zhang G, Wang Z, Zhu P, et al. circREEP3 drives colorectal cancer progression via activation of FKBP10 transcription and restriction of antitumor immunity. Adv Sci. 2022;9(13):e2105160. [CrossRef].
3. Fadlallah H, El Masri J, Fakhereddine H, Youssef J, Chemaly C, Doughan S, et al. Colorectal cancer: recent advances in management and treatment. World J Clin Oncol. 2024;15(9):1136–56. [CrossRef].
4. Komatsu M, Ichikawa H, Chiwaki F, Sakamoto H, Komatsuzaki R, Asaumi M, et al. ARHGAP-RhoA signaling provokes homotypic adhesion-triggered cell death of metastasized diffuse-type gastric cancer. Oncogene. 2022;41(43):4779–94. [CrossRef].
5. Liu W, Xia K, Zheng D, Huang X, Wei Z, Wei Z, et al. Construction of a prognostic risk score model based on the ARHGAP family to predict the survival of osteosarcoma. BMC Cancer. 2023;23(1):1179. [CrossRef].
6. Géci I, Bober P, Filová E, Amler E, Sabo J. The role of ARHGAP1 in Rho GTPase inactivation during metastasizing of breast cancer cell line MCF-7 after treatment with doxorubicin. Int J Mol Sci. 2023;24(14):11352. [CrossRef].
7. Johnstone CN, Castellví-Bel S, Chang LM, Bessa X, Nakagawa H, Harada H, et al. ARHGAP8 is a novel member of the RHOGAP family related to ARHGAP1/CDC42GAP/p50RHOGAP: mutation and expression analyses in colorectal and breast cancers. Gene. 2004;336(1):59–71. [CrossRef].
8. Wang J, Qian J, Hu Y, Kong X, Chen H, Shi Q, et al. ArhGAP30 promotes p53 acetylation and function in colorectal cancer. Nat Commun. 2014;5:4735. [CrossRef].
9. Yu N, Yuan B, Cai J, Liu J, Zhang W, Bao W, et al. Loss of ARHGAP40 expression in basal cell carcinoma via CpG island hypermethylation. Exp Dermatol. 2023;32(12):2094–101. [CrossRef].
10. Huang H, Wang S, Guan Y, Ren J, Liu X. Molecular basis and current insights of atypical Rho small GTPase in cancer. Mol Biol Rep. 2024;51(1):141. [CrossRef].
11. Zhang GY, Yang WH, Chen Z. Upregulated STAT3 and RhoA signaling in colorectal cancer (CRC) regulate the invasion and migration of CRC cells. Eur Rev Med Pharmacol Sci. 2016;20(10):2028–37.

12. Ding AX, Wang H, Zhang JM, Yang W, Kuang YT. lncRNA BANCR promotes the colorectal cancer metastasis through accelerating exosomes-mediated M2 macrophage polarization via regulating RhoA/ROCK signaling. Mol Cell Biochem. 2024;479(1):13–27. [CrossRef].
13. Darsaut TE, Rheaume AR, Chagnon M, Raymond J. The use and abuse of survival analysis and Kaplan-Meier curves in surgical trials. Neurochirurgie. 2024;70(4):101567. [CrossRef].
14. Ruihua H, Mengyi Z, Chong Z, Meng Q, Xin M, Qiulin T, et al. RhoA regulates resistance to irinotecan by regulating membrane transporter and apoptosis signaling in colorectal cancer. Oncotarget. 2016;7(52):87136–46. [CrossRef].
15. Lu L, Wu M, Lu Y, Zhao Z, Liu T, Fu W, et al. MicroRNA-424 regulates cisplatin resistance of gastric cancer by targeting SMURF1 based on GEO database and primary validation in human gastric cancer tissues. Onco Targets Ther. 2019;12:7623–36. [CrossRef].
16. Jeong D, Park S, Kim H, Kim CJ, Ahn TS, Bae SB, et al. RhoA is associated with invasion and poor prognosis in colorectal cancer. Int J Oncol. 2016;48(2):714–22. [CrossRef].
17. Xin R, Tang XM, Jiang YJ, Yu F, Li S, Jia CY, et al. Construction of a novel MYC-associated ceRNA regulatory network to identify prognostic biomarkers in colon adenocarcinoma. J Oncol. 2022;2022:3216285. [CrossRef].
18. Yang C, Wu S, Mou Z, Zhou Q, Zhang Z, Chen Y, et al. Transcriptomic analysis identified ARHGAP family as a novel biomarker associated with tumor-promoting immune infiltration and nanomechanical characteristics in bladder cancer. Front Cell Dev Biol. 2021;9:657219. [CrossRef].
19. Qi L, Sun B, Yang B, Lu S. circRNA RPPH1 facilitates the aggravation of breast cancer development by regulating miR-542-3p/ARHGAP1 pathway. Cancer Biother Radiopharm. 2022;37(8):708–19. [CrossRef].
20. Ke H, Shao J, Hu J, Song X, Han H, Zhu Z, et al. ARHGAP10, transcriptionally regulated by sodium butyrate, promotes ferroptosis of ovarian cancer cells. Front Biosci. 2024;29(5):167. [CrossRef].
21. Meng B, Wang P, Zhao C, Yin G, Meng X, Li L, et al. miR-21-5p serves as a promoter in renal cell carcinoma progression through ARHGAP24 downregulation. Environ Sci Pollut Res Int. 2022;29(26):39985–93. [CrossRef].
22. Yang W, Wang B, Yu Q, Liu T, Li T, Tian T, et al. ARHGAP24 represses β-catenin transactivation-induced invasiveness in hepatocellular carcinoma mainly by acting as a GTPase-independent scaffold. Theranostics. 2022;12(14):6189–206. [CrossRef].
23. Guo F, Liu Y, Huang J, Li Y, Zhou G, Wang D, et al. Identification of Rho GTPase activating protein 6 isoform 1 variant as a new molecular marker in human colorectal tumors. Pathol Oncol Res. 2010;16(3):319–26. [CrossRef].
24. Hossain MJ, Chowdhury UN, Islam MB, Uddin S, Ahmed MB, Quinn JMW, et al. Machine learning and network-based models to identify genetic risk factors to the progression and survival of colorectal cancer. Comput Biol Med. 2021;135:104539. [CrossRef].
25. Fu MS, Pan SX, Cai XQ, Hu YX, Zhang WJ, Pan QC. Analysis of ARHGAP4 expression with colorectal cancer clinical characteristics and prognosis. Front Oncol. 2022;12:899837. [CrossRef].
26. Zhou X, Liu Z, He T, Zhang C, Jiang M, Jin Y, et al. DDX10 promotes the proliferation and metastasis of colorectal cancer cells via splicing RPL35. Cancer Cell Int. 2022;22(1):58. [CrossRef].
27. Townsend AR, Chong LC, Karapetis C, Price TJ. Selective internal radiation therapy for liver metastases from colorectal cancer. Cancer Treat Rev. 2016;50:148–54. [CrossRef].
28. Streets AJ, Prosseda PP, Ong AC. Polycystin-1 regulates ARHGAP35-dependent centrosomal RhoA activation and ROCK signaling. JCI Insight. 2020;5(16):e135385. [CrossRef].
29. Zhao A, Zhu X, Wu H, Wang J, Zhang M, Xiang J, et al. B7-H3 promotes the migration and invasion of colorectal cancer cells via regulating the actin cytoskeleton and RhoA/ROCK1/LIMK1 signaling pathway. Tissue Cell. 2024;90:102518. [CrossRef].
30. Rodrigues P, Macaya I, Bazzocco S, Mazzolini R, Andretta E, Dopeso H, et al. RHOA inactivation enhances Wnt signalling and promotes colorectal cancer. Nat Commun. 2014;5:5458. [CrossRef].
31. Pan S, Deng Y, Fu J, Zhang Y, Zhang Z, Ru X, et al. Decreased expression of ARHGAP15 promotes the development of colorectal cancer through PTEN/AKT/FOXO1 axis. Cell Death Dis. 2018;9(6):673. [CrossRef].
32. Zhang S, Sui L, Zhuang J, He S, Song Y, Ye Y, et al. ARHGAP24 regulates cell ability and apoptosis of colorectal cancer cells via the regulation of P53. Oncol Lett. 2018;16(3):3517–24. [CrossRef].
33. Jaffe AB, Hall A. Rho GTPases: biochemistry and biology. Annu Rev Cell Dev Biol. 2005;21:247–69. [CrossRef].

34. Moissoglu K, Kiessling V, Wan C, Hoffman BD, Norambuena A, Tamm LK, et al. Regulation of Rac1 translocation and activation by membrane domains and their boundaries. J Cell Sci. 2014;127(Pt 11):2565–76. [CrossRef].
35. Spindler V, Schlegel N, Waschke J. Role of GTPases in control of microvascular permeability. Cardiovasc Res. 2010;87(2):243–53. [CrossRef].
36. Tian T, Chen ZH, Zheng Z, Liu Y, Zhao Q, Liu Y, et al. Investigation of the role and mechanism of ARHGAP5-mediated colorectal cancer metastasis. Theranostics. 2020;10(13):5998–6010. [CrossRef].
37. Sekiguchi M, Sobue A, Kushima I, Wang C, Arioka Y, Kato H, et al. ARHGAP10, which encodes Rho GTPase-activating protein 10, is a novel gene for schizophrenia risk. Transl Psychiatry. 2020;10(1):247. [CrossRef].
38. Kasuya K, Nagakawa Y, Hosokawa Y, Sahara Y, Takishita C, Nakajima T, et al. RhoA activity increases due to hypermethylation of ARHGAP28 in a highly liver-metastatic colon cancer cell line. Biomed Rep. 2016;4(3):335–9. [CrossRef].